X-ray Absorption Spectroscopic Studies at the Cobalt K-Edge on a Reduced Al_2O_3-Supported Rhenium-Promoted Cobalt Fischer−Tropsch Catalyst

Arild Moen† and David G. Nicholson*

Department of Chemistry, Norwegian University of Science and Technology, N-7055 Trondheim, Norway

Bjerne S. Clausen, Poul L. Hansen, Alfons Molenbroek, and Gert Steffensen

Haldor Topsøe Research Laboratories, DK-2800, Lyngby, Denmark

Received December 4, 1996. Revised Manuscript Received February 26, 1997[⊗]

In situ XAFS spectroscopic studies have been carried out at 450 °C on the hydrogen reduction of a rhenium-promoted Co_3O_4/Al_2O_3 catalyst. The results show that reduction at this temperature yields a highly dispersed system with small cobalt metal particles (<40 Å). In addition, a lower fraction of the cobalt content is randomly dispersed over the tetrahedral vacancies of the alumina support. This dispersion occurs during reduction and not calcination. The cobalt in these sites cannot be reduced at 450 °C, a temperature that is too low to permit formation of the spinel $CoAl_2O_4$. A particularly significant feature of the spectrum of the reduced material is that the energy of the K-edge is increased by 3−4 eV. This is attributed to the small size of the metal particles and consequently a deviation from bulk properties. The effect is a manifestation of changes in shielding of the 1s electrons by the valence orbitals relative to the situation pertaining to the bulk metal. The actual crystal form of the metal particles could not be determined, but the recently reported metastable non-close-packed body-centered cubic form cannot be excluded, especially since graphite was present and carbon is suggested to catalyze transformation to this structure.

The synthesis of hydrocarbons is an important stage in converting natural gas to petrochemicals. This is exemplified by the Fischer−Tropsch process in which linear high-molecular-weight aliphatic hydrocarbons are synthesized by catalytically hydrogenating carbon monoxide using alumina-supported cobalt as the catalyst.[1−28] The paper by Holmen et al.[28] contains a comprehensive review of the recent literature concerning this system and its variations.

The picture that emerges from these studies is one in which catalyst preparation involves the diffusion of cobalt ions into the structure of γ-Al_2O_3, where they occupy vacant octahedral and/or tetrahedral positions. This appears to result in two main types of cobalt-containing phase: (a) cobalt bonded to the alumina support in the form of a surface phase that is resistant to reduction and (b) the easily reduced spinel Co_3O_4 which dominates above a certain cobalt concentration (ca. 2%). The relative amounts of these phases depend on the temperature of calcination as well as on the cobalt concentration. An important factor which has to be taken into account is the different temperatures at which reduction takes place for these cobalt-containing phases. Another factor is the influence of promotors; it is known that the rates of hydrogenation of carbon

† Present address: Department of Chemistry, Centre for Research on Interface Properties and Catalysts, Laval University, Ste-Foy, G1K 7P4 Quebec, Canada.

⊗ Abstract published in *Advance ACS Abstracts,* April 1, 1997.

(1) Ashley, J. H.; Mitchell, P. C. H. *J. Chem. Soc.,* A **1968**, 2821.
(2) Asmolov, G. N.; Krylov, O. V. *Kinet. Katal.* **1971**, *12*, 463.
(3) Ueda, H.; Todo, N. *J. Catal.* **1972**, *27*, 281
(4) Jacono, M. Lo.; Verbeek, J. L.; Schuit, G. C. A. *J. Catal.* **1973**, *29*, 463.
(5) Grimblot, J.; Bonnelle, J. P.; Beaufils, J. P. *J. Electron Spectrosc. Relat. Phenom* **1976**, *8*, 473.
(6) Declerck-Grimée, R. I.; Caresson, R. M.; Friedman, R. M.; Fripiat, J. J. *J. Phys. Chem.* **1978**, *83*, 885.
(7) Dufresne, P.; Grimblot, J.; Bonnelle, J. P. *Bull. Soc. Chim. Fr.* **1980**, *1*, 89.
(8) Chung, K. S.; Massoth, F. E. *J. Catal.* **1980**, *64*, 320.
(9) Chung, K. S.; Massoth, F. E. *J. Catal.* **1980**, *64*, 332.
(10) Greegor, R. B.; Lytle, F. W.; Chin, R. L.; Hercules, D. M. *J. Phys. Chem.* **1981**, *85*, 1232.
(11) Topsøe, H.; Clausen, B. S.; Candia, R.; Wivel, C. *J. Catal.* **1981**, *68*, 433.
(12) Topsøe, N.; Topsøe, H. *J. Catal.* **1982**, *75*, 354.
(13) Chin, R. L.; Hercules, D. M. *J. Phys. Chem.* **1982**, *86*, 360.
(14) Alstrup, I.; Chorkendorf, I.; Candia, R.; Clausen, B. S.; Topsøe, H. *J. Catal.* **1982**, *77*, 397
(15) Wivel, C.; Clausen, B. S.; Candia, R.; Mørup, S.; Topsøe, H. *J. Catal.* **1984**, *87*, 497.
(16) Arnoldy, P.; Massoth, F. E. *J. Catal.* **1985**, *93*, 38.
(17) Stanick, M. A.; Houalla, M.; Hercules, D. *J. Catal.* **1987**, *103*, 151.
(18) Garbowski, E.; Guenin, M.; Marion, M.; Primet, M. *Appl. Catal.* **1990**, *64*, 209.
(19) Tung, H. C.; Yeh, C.; Hong, C. T. *J. Catal.* **1990**, *122*, 211.
(20) Bai, C.; Soled, S.; Dwight, K; Wold, A. *J. Solid State Chem.* **1991**, *91*, 148.
(21) Fay, M. J.; Procter, A.; Hoffmann, D. P.; Houalla, M.; Hercules, D. M. *Appl. Spetrosc.* **1992**, *46*, 345.
(22) Blekkan, E. A.; Holmen, H.; Vada, S. *Acta Chem. Scand.* **1993**, 47, 275.
(23) Shirai, M.; Inoue, T.; Onishi, H.; Asakura, K.; Iwasawa, Y. *J. Catal.* **1994**, *145*, 159.
(24) Senden, M. M. G.; Sie, S. T.; Post, M. F. M.; Ansorge, J. In *Chemical Reactor Technology for Environmentally Safe Reactors and Products*; Lasa, de H. I., Dogu, G., Ravella, A., Eds.; Kluwer: Dordrecht, 1992; p 227.
(25) Dimitrova, P. G.; Mehandjiev, D. R. *J. Catal.* **1994**, *145*, 356.
(26) Vada, S.; Hoff, A.; Ådnanes, E.; Schanke, D.; Holmen, A. *Top. Catal.* **1995**, *2*, 155.
(27) Schanke, D.; Hilmen, A. M.; Bergene, E.; Kinnari, K.; Rytter, E.; Ådnanes, E.; Holmen, A. *Catal. Lett.* **1995**, *34*, 269.
(28) Hilman, A. M.; Schanke, D.; Holmen, A. *Catal. Lett.* **1996**, *34*, 143.

S0897-4756(96)00619-9 CCC: $14.00

monoxide are increased 2-fold by platinum- and rhenium promoters.[25,26]

Catalytic activity is governed by the local geometric, and hence electronic structure, of the active sites. It is therefore necessary to ascertain the immediate environments about these sites if catalytic behavior is to be satisfactorily rationalized. In the case of the present catalyst, it is known that activation involves reduction to the metal, but this seemingly simple material is actually quite complex because several structural forms or polytypes can be involved in the catalytic process (see below). It is important to identify both the form and dimensions of the particular variation of the system. The dimensions or dispersion of the metal clusters or crystallites are factors crucial to the efficacy of the catalyst. As the size of the metal particles decreases (below ca. 100 Å for spheres) the average environment of the metal atoms deviates more and more from that in the bulk metal itself simply because more of the atoms are progressively closer to the surface and the physical properties deviate increasingly from those of the bulk. Crystal structure is relevant because catalytic behavior is connected to active sites on specific crystal planes.

X-ray absorption spectroscopy (XAS) is valuable for studying the local structure around selected sites in heterogeneous catalysts. Heterogeneous catalysts are essentially involved in chemical reactions at surfaces, and although XAS is actually a bulk technique, the overall contribution to the XAS signal is considerable because a significant proportion of the active sites are highly dispersed over a large number of surfaces. Indeed, XAS is particularly well suited for characterizing highly dispersed systems because the lack of sufficient long-range order makes them not amenable to X-ray diffraction. Moreover, the technique can also give information on interactions between the support and the metal catalyst. Such interactions are known to influence activity and selectivity.[29−32]

XAS has previously been used to study modifications of the Co/Al_2O_3 catalysts. Fay et al.[21] used the method to characterize a boron-modified system, and recently Huffman et al.[33] reported studies using in situ XAS applied to potassium-promoted cobalt catalysts supported on Al_2O_3 and SiO_2 during reduction in hydrogen at 200 °C and subsequent reaction in a synthesis gas mixture. The latter support was also used by Takeuchi et al.[34]

There are no previous reports of XAS studies on the rhenium-promoted system and we report here the results of a higher temperature (450 °C) in situ XAS study at the Co K edge on the hydrogen reduction of a rhenium-promoted Co/Al_2O_3 catalyst.

Experimental Section

Synthesis. Essentially following the procedure described in detail in the literature[26] (but with a triple cobalt loading) the alumina-supported cobalt catalyst with 26% cobalt loading (analysis by atomic absorption spectroscopy) was prepared by the incipient wetness impregnation of γ-alumina (sieved to 40−50 mesh) with aqueous solutions of $Co(NO_3)_2 \cdot 6H_2O$ and $HReO_4$ (calculated to give 1.0 wt % rhenium). The resulting material was dried overnight at 120 °C and then calcined at 500 °C for 8 h. Hydrogen reduction of the catalyst was carried out in situ (see below). The nonreduced and reduced samples are designated sample A and sample B, respectively.

X-ray Absorption Data Collection. XAS data were collected using the facilities of the Daresbury Synchrotron Radiation Source (SRS) and HASYLAB, DESY, Hamburg, with synchrotron radiation from the DORIS III storage ring. Spectra were obtained on stations 7.1 (Daresbury) and X1-Römo II (HASYLAB) at the cobalt K-edge ($\lambda = 1.6086$ Å, energy = 7709 eV).

Double-crystal silicon (111) and (311) monochromators were used to scan the X-ray spectra at Daresbury and HASYLAB, respectively. Ion chambers were used at both facilities for detecting the intensities of the incident and transmitted X-rays. At Daresbury the first ion chamber was filled with 20% argon (31 Torr) and the second ion chamber with 78% argon (224 Torr) and both chambers filled to atmospheric pressure with helium. The HASYLAB ion chambers were filled with nitrogen.

The experiments were performed with electron beam energies of 2.0 and 4.455 GeV and maximum stored currents of 205 and 100 mA for Daresbury and HASYLAB, respectively. The harmonic rejection for both data collections was set to 50%.

Data Collected at the Co K-Edge. At Daresbury, energy calibration of the XAS was effected by inserting Co foil (thickness 5 μm; K-edge 7709 eV) between the second and a third ionization chamber and measuring both spectra simultaneously. Accurate energy scale calibration was carried out later using an in-house program. A similar setup was used at HASYLAB except that the reference was Eu_2O_3 (L_{III}-edge 6985 eV, accuracy ±0.1 eV). The XAS of the unreduced catalyst and the model compounds $CoAl_2O_4$, CoO, the cobalt Tutton salt, $(NH_4)_2[Co(H_2O)_6](SO_4)_2$, and Co_3O_4 were measured at Daresbury; the reduced catalyst and the model compounds cobalt Tutton salt and $CoAl_2O_4$ were measured at HASYLAB. The amounts of material in the samples for XAS were calculated from element mass fractions and the absorption coefficients of the constituent elements[35] just above the absorption edge to give an absorber optical thickness of 1.5 absorption lengths.

For the Daresbury experiments, the well-powdered samples were mixed with boron nitride so as to give a sample thickness of ca. 1.0 mm and placed in aluminum sample holders and held in place by Kapton tape. The HASYLAB samples other than the in situ sample were in the form of disks prepared by pressing the requisite amount of sieved (7−125 μm) material with polyethylene powder in a 16 mm diameter die. After drying and calcining (see above), Co_3O_4/Al_2O_3 destined for the in situ reduction was ground, sieved, and mixed with the requisite amount of graphite to achieve the desired absorber thickness (see above). The catalyst was then loaded into the in situ reactor cell[36] and reduced in H_2 by heating from room temperature to 450 °C and maintaining at that temperature for 6 h.

EXAFS Data Analysis. The data were corrected for dark currents, converted to k-space, summed, and background subtracted to yield the EXAFS function $\chi^{obs}{}_i(k)$ using the *EXCALIB* and *EXBACK* programs.[36] Model fitting was carried out with *EXCURV90* using curved-wave theory and ab initio phase shifts.[38]

The EXAFS spectra were least-squares fitted using k^1 and k^3 weighted data. Optimizing the k^1 and k^3 fits has been shown to reduce coupling between N (multiplicity) and $2\sigma^2$ (Debye−Waller-type factor) and also between r (distance) and E_0 (magnitude of the photoelectron energy at $k = 0$) and gives a solution common to both weighting schemes.[39] Results consistent with these were also obtained by means of correla-

(29) Moen, A. Ph.D. Thesis, University of Trondheim, 1995.
(30) Solymosi, F. *Catal. Rev.* **1968**, *1*, 233.
(31) LoJacono M.; Schiavello, M. *Preparation of Catalysts;* Delmon, B., Jacobs, P. A., Poncelot, G., Eds.; Elsevier: Amsterdam, 1976; p 473
(32) Reuel, R. C.; Bartholomew, C. H. *J. Catal.* **1984**, *85*, 78.
(33) Huffman, G. H.; Shah, N.; Zhao, J.; Huggins, F. E.; Hoost, T. E.; Halvorsen, S.; Goodwin, J. G. *J. Catal.* **1995**, *151*, 17.
(34) Takeuchi, K.; Hanaoka, T.; Matsuzaki, T.; Reinikainen, M.; Sugi, Y. *Catal. Lett.* **1991**, 8, 253.
(35) International Tables for X-ray Crystallography; Kynick Press: Birmingham, 1962; Vol. 3, p 175.
(36) Clausen, B. S.; Topsoe, H. *Catal. Today* **1991**, *9*, 189.

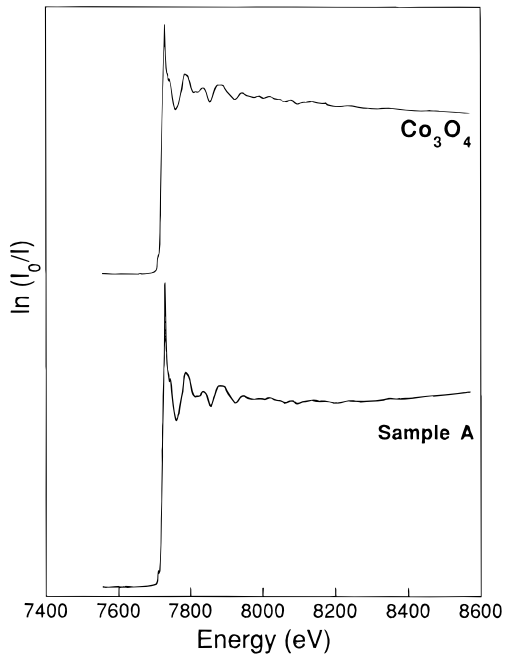

Figure 1. Normalized XAS of sample A and the reference compound Co_3O_4.

tion maps between the above pairs of parameters. The k^3 weighting scheme compensates for the diminishing photoelectron wave at higher k. The curve-fitting was performed on data that had been Fourier filtered over a wide range (1.0−25.0 Å). This filter removes low-frequency contributions to the EXAFS below 1 Å, but does not smooth the spectrum (i.e., the noise is not removed). Only those shells significant at the 99% level[40] were included in the final fits.

The model compounds, cobalt Tutton salt,[41] cobalt aluminate,[42] and cobalt(II) oxide[43] were used to check the validity of the ab initio phase shifts and establish the general parameters, *AFAC* (proportion of absorption causing EXAFS) and *VPI* (allows for inelastic scattering of the photoelectron).[38] The cobalt spinel (Co_3O_4), which contains both cobalt(II) and cobalt(III),[44] was used as a reference.

Multiple scattering (MS) effects are important for some of the shells in the spinel structures, cobalt(II) oxide, and cobalt metal because of collinear arrangements of atoms.

Results and Discussion

Figure 1 shows that the XAS of the unreduced material (sample A) cannot be distinguished from that of the reference compound Co_3O_4. This is more easily seen in Figure 2 which depicts the Fourier transforms of the EXAFS of Co_3O_4, $CoAl_2O_4$, and sample A.

It is clear that the preparation, together with the comparatively high cobalt loading, yields a material in which Co_3O_4 is the dominant phase (see Introduction) and that this phase is distributed throughout sample A in the form of relatively large (>100 Å) crystallites. This conclusion is supported by the line broadening observed in the X-ray diffractogram which shows that the sizes of the Co_3O_4 crystallites are in the range 140−190 Å.[26]

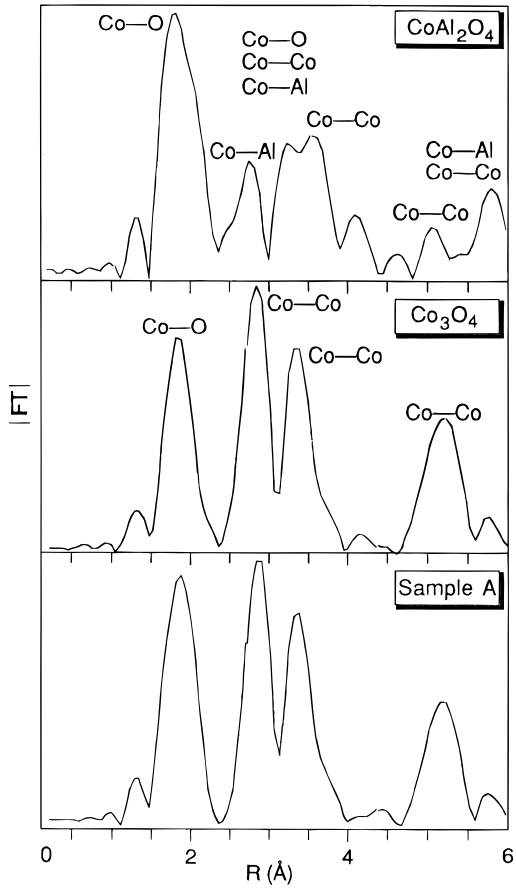

Figure 2. Fourier transforms of sample A and the reference compounds Co_3O_4 and $CoAl_2O_4$.

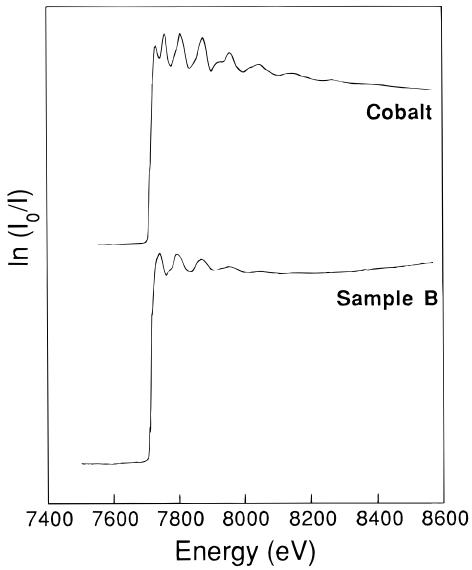

Figure 3. Normalized XAS of sample B and bulk cobalt metal.

Figures 3 and 4 show the XAS of the reduced material (sample B) and bulk cobalt metal and the X-ray absorption near edge structure (XANES) region for samples A and B and the model/reference compounds. The latter have been chosen for their tetrahedral and octahedral cobalt environments as represented by the following

(37) EXCALIB, EXBACK, and EXCURV90 programs: Binsted, N.; Campbell, J. W.; Gurman, S. J.; Stephenson, P. C. SERC Daresbury Laboratory, 1990.
(38) Gurman, S. J.; Binsted, N.; Ross, I. *J. Phys.* **1984,** *C17*, 143.
(39) Kampers, F. W. H. Ph.D. Thesis, Eindhoven University of Technology, 1988.
(40) Joyner, R. W.; Martin, K. J.; Meehan, P. *J. Phys. C: Solid State Phys.* **1987**, *20*, 4005.
(41) Cotton, F. A.; Daniels, L. M.; Murillo, C. A.; Quesada, J. F. *Inorg. Chem.* **1993**, *32*, 4861.
(42) Toriuma, K.; Ozima, M.; Akaogi, M.; Sato, Y. *Acta Crystallogr.*, B **1978**, *34*, 1093.
(43) Sasaki, S.; Fujino, K.; Takeuchi, Y. *Proc. Jpn. Acad.* **1979**, *55B*, 43.
(44) Greenwood, N. N.; Earnshaw, A. *Chemistry of the Elements*; Pergamon Press: New York, 1984; p 1294.

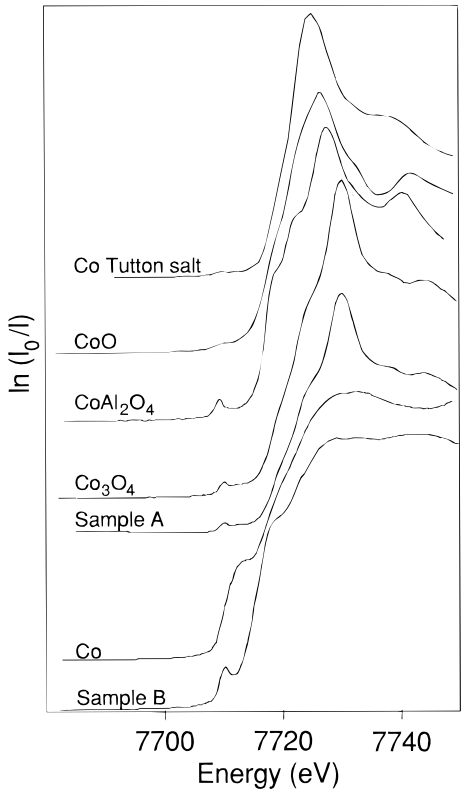

Figure 4. Normalized Co K-edge XANES of samples A and B and the reference compounds, cobalt metal, Co_3O_4, $CoAl_2O_4$, CoO, and the Tutton salt $(NH_4)_2[Co(H_2O)_6](SO_4)_2$.

compounds: $CoAl_2O_4$ (tetrahedral $Co^{II}(O)_4$); $(NH_4)_2[Co(H_2O)_6](SO_4)_2$ (distorted octahedral $Co^{II}(O)_6$); CoO (octahedral $Co^{II}(O)_6$); and Co_3O_4 (tetrahedral $Co^{II}(O)_4$) plus octahedral $Co^{II}(O)_6$). Figure 5 contains the first derivatives of the edge region because these are useful for highlighting characteristic features about the edges (particularly the preedge features) and establishing their energies.

Huffman et al.[33] reported that reduction of potassium-promoted Co_3O_4/Al_2O_3 at 200 °C yields cobalt metal particles in which the coordination numbers are less than those for bulk cobalt metal. On this basis they estimated the average particle size to be as small as 10–20 Å. The authors doubted this estimate noting that the actual size must be larger. Unlike the present work, no other cobalt-containing phase was detected.

A comparison of the XAS of cobalt metal (as a foil) and sample B in Figure 3 reveals major differences. This also applies to the edge regions of bulk cobalt metal and sample B, which are emphasized by the first derivatives (Figure 5). To facilitate the contrast, the XANES regions for bulk cobalt metal, sample A and sample B are overlaid in Figure 6. Clearly sample B does not contain bulklike crystallites of cobalt metal.

The most prominant features of the XAS of sample B are the preedge peak at 7709 eV and the absence of the whiteline that is characteristic of Co_3O_4, $CoAl_2O_4$, CoO, cobalt Tutton salt, and sample A. The white line is also absent in the XAS of bulk cobalt metal which suggests that sample B contains a high degree of reduced material consistent with the estimate (80%) for reducibility of rhenium-promoted Co_3O_4/Al_2O_3 under the same conditions.[26]

Preedge peaks. The XAS at the K-edge of certain valence states of some transition compounds often

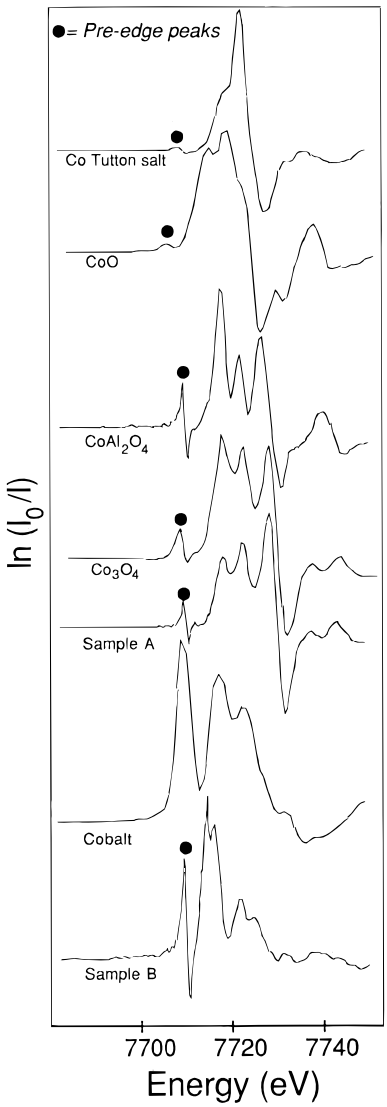

Figure 5. First derivatives of the XANES region of samples A and B and the reference compounds, cobalt metal, Co_3O_4, $CoAl_2O_4$, CoO, and the Tutton salt $(NH_4)_2[Co(H_2O)_6](SO_4)_2$. The derivatives of the preedge features are marked (●).

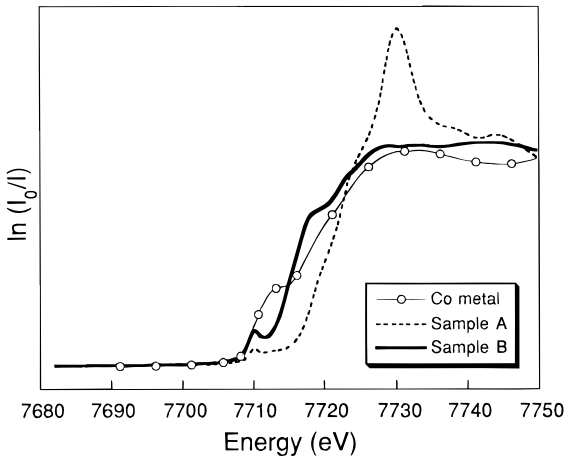

Figure 6. Normalized Co K-edge XANES regions of samples A and B and the reference cobalt metal (bulk).

contain an electronically interesting preedge feature a few electronvolts below the edge. This feature is useful because it yields structural and electronic information—especially when combined with the extended X-ray absorption fine structure (EXAFS) region of the same

spectrum.[45] The peak results from the absorption process *1*s → 3d and for solid macromolecular materials (such as CoO, $CoAl_2O_4$, and Co_3O_4) the final state(s) are unoccupied bands. The transition probability (intensity) is related to the symmetry ($A_1 \rightarrow T_2$ for T_d symmetry) and to the occupancy of the 3d shell. For a given occupancy, the transition is most intense when the first coordination shell lacks inversion symmetry. In the case of the cubic point groups this applies to tetrahedral (T_d) environments but not to octahedral (O_h) symmetry; although for the latter point group a considerably weaker preedge feature does actually occur (despite being forbidden by the center of symmetry). This is because the crystallographic point group represents a static model derived by time-averaging the asymmetric vibrations within the molecule whereas the XAS reacts to the individually and constantly changing structures of the local environment because vibrations momentarily eliminate the center of symmetry. An example is the spectrum (Figures 4 and 5) of CoO, with its very weak preedge feature (better revealed in the derivative of the spectrum), in which the octahedrally coordinated cobalt is in an O_h environment.[43]

For symmetries lower than O_h, as in the distorted octahedrally coordinated cobalt environment ($Co(H_2O)_6^{2+}$) in the Tutton salt, $Co(NH_4)_2(SO_4)_2 \cdot 6H_2O$,[41] the intensity is somewhat enhanced, although still comparatively weak.

In contrast, the preedge peaks associated with tetrahedral cobalt environments are more intense in accordance with the noncentrosymmeric T_d point group. This is exemplified in the spectrum of $CoAl_2O_4$ (Figures 4 and 5).

These figures also show the preedge region for the spinel Co_3O_4 with one-third cobalt(II) in tetrahedral sites and two-thirds Co(III) in octahedral sites. The preedge feature is composed of the tetrahedral peak and the very weak (forbidden) octahedral peak, the overall peak intensity being reduced because the proportion of the cobalt content in tetrahedral sites is now only one third the total cobalt content and not unity as in $CoAl_2O_4$ (but see below).

XAS of Sample B. In sample B the preedge peak at 7710 eV is a particularly important diagnostic feature because it indicates that tetrahedral $Co^{II}(O)_4$ environments are present while the absence of the white line is characteristic of metallic cobalt. Since the edge energy of bulk metallic cobalt is 7709 eV, any significant fraction of the metal XAS in a two-or-more phase composite spectrum would obscure this preedge peak. This does not occur here because the edge is actually moved to a higher energy (7714 eV). The edge positions (±1.0 eV) for a selection of calibrated cobalt environments are CoO 7719, Co_3O_4 (Co(II) and Co(III)) 7722; $CoAl_2O_4$ 7722 (mainly tetrahedral Co(II) but with a minor distribution (0.155) of cobalt in the octahedral sites[42]), and the Tutton salt 7222 eV. It is evident that the edge energy of sample B is relatively low; it is an interesting feature that sets it apart from all of the other compounds. This anomalous position is connected to the valence states of cobalt.

Variations in K-edge positions reflect shielding of the 1s orbital from the nucleus by the valence electron density. The latter is complicated by a complex interplay of various factors that can lead to chemical bond differences affecting edge positions more than formal valence states. This is illustrated by the difference in edge energy for the two octahedral Co(II) environments in CoO and the Tutton salt. A key observation (discussed below) is that the edge energy for sample B (although low compared with the energies of the reference compounds) is significantly higher than that for the bulk metal.

At first sight, the information on sample B given by both the preedge peak and the absence of a sharp white line appear to conflict. Whereas the former indicates a significant oxide:metal ratio the latter suggests that the metal:oxide ratio is high. Simulating the region directly about the edge by summing a range of ratios of the Co foil and $CoAl_2O_4$ spectra shows that concentrations of cobalt metal from a minimum of ca. 40% yield composite spectra in which the preedge feature of sample B is completely obscured. If the absence of the white line is to be replicated then large (>80%) metal components are required. It is only possible to simulate both features in sample B if the cobalt foil component spectrum is shifted by 3−4 eV to higher energy before summing with the $CoAl_2O_4$ contribution.

The modulus of the Fourier transform of the EXAFS of sample B is shown in Figure 7, together with that for the bulk metal. The considerably lower magnitude of the transform of the former, which reflects the low amplitude of the EXAFS, indicates small particle sizes. This is because a significant fraction of the cobalt atoms are positioned at, or near, the surface of very small particles. It is not possible to attain a good fit of the EXAFS using a harmonic model of disorder (Debye−Waller factor). This is also consistent with small particle sizes because the overall anharmonic signal arises from component signals for individual distances contained within a range.

Hence, in sample B, a minor fraction of cobalt is placed in the tetrahedral environment that we know is present from the preedge peak; this contribution to the EXAFS broadens the Fourier peak. The distances extracted from the EXAFS are 1.92 ± 0.03 Å for the $Co(O)_4$ tetrahedral site and 2.49 ± 0.03 Å due to Co−Co backscattering. Whereas the former distance corresponds to the bond length of a tetrahedral $Co^{II}(O)_4$ environment, the latter distance is the same as that in all of the forms of cobalt metal (see below). The absence of significant contributions from more distant Co···Co shells is also consistent with small particle sizes.

Nonmetallic Phase. It has been assumed that $CoAl_2O_4$ is the phase generated when cobalt occupies the vacant tetrahedral positions of the alumina lattice[25] but the EXAFS here clearly excludes the presence of $CoAl_2O_4$ in sample B (see Figures 2, 5, and 7) because the Co···Co distance in that compound is considerably longer (2.83 Å).[42] Instead, it is evident that only a small fraction of the total cobalt content of sample B is randomly dispersed over vacant tetrahedral sites of the alumina support. This conclusion is supported by an X-ray diffraction study[49] which also shows that $CoAl_2O_4$

(45) Moen, A.; Nicholson, D. G.; Rønning, M. *J. Chem. Soc., Faraday Trans.* **1995**, *91*, 3189 and references therein.

(46) Donohue, J. *The structure of the Elements*; Wiley: New York, 1974; p 207 and references therein.

(47) Colley, S. E.; Copperthwaite, R. G.; Hutchings, G. J.; Terblanche, S. P.; Thackeray, M. M. *Nature* **1989,** *339*, 129.

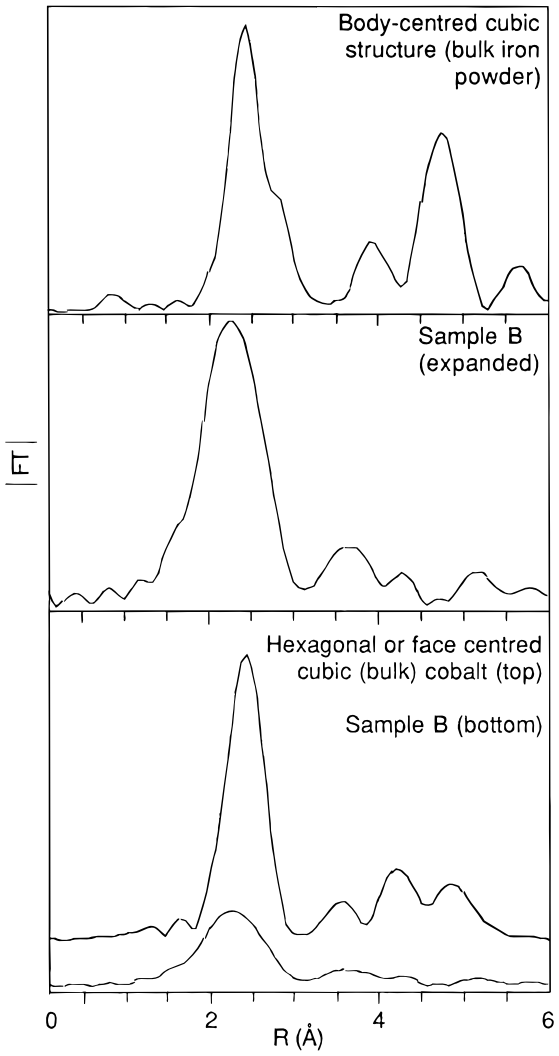

Figure 7. Fourier transforms of (a) body-centered cubic bulk iron powder; (b) sample B with expanded amplitude scale; (c) sample B and bulk hexagonal cobalt metal on the same amplitude scale.

is not formed and additionally by the observation[25] that much higher calcination temperatures (>1200 °C) are needed to form $CoAl_2O_4$ from mixtures of Co_3O_4 and Al_2O_3.

Major Cobalt-Containing Phase in Sample B. Neglecting for the moment the shift in edge energy, it is evident from the reduced EXAFS amplitude that sample B contains very small particles of metallic cobalt as the major cobalt-containing fraction. This supports the conclusion of Holmen et al.[26] that 78% of the cobalt content of the reduced material is in the form of the metal. Temperature-programmed reduction studies[27] show that diffusion into alumina occurs during reduction and not calcination. The effect of particle size on the EXAFS amplitude is significant for dimensions below ca. 30 Å.[23] Recent studies on the size determination by EXAFS confirm this.[50] Copper clusters produced by ion implantation in AlN with sizes ranging from 9 to 40 Å show that EXAFS is insensitive to the size of clusters with more than 2000 atoms (25 Å). The amplitude reduction exhibited in the EXAFS by copper particles <25 Å is similar to that shown for the cobalt particles in sample B. This would indicate cobalt particles even smaller than those (perhaps conservatively) estimated here.

Of course, the presence of metallic cobalt as the major component in sample B needs to be reconciled with the aforementioned shift in edge energy. Since this must be rooted in the special nature of these particular metal particles we consider now some of the structural characteristics of metallic cobalt and the implications particle size has on the XAS. It is also necessary to consider the recently reported metastable noncubic close-packed form of cobalt.

Structural Forms of Cobalt. Cobalt appears to exist in the three forms: hexagonal close-packed (hcp), cubic close-packed (face-centered cubic, fcc) and cubic non-close-packed (body-centered cubic, bcc). The latter, which has only recently been reported (see below), may be relevant to the present study. It is important to establish the structural identity of the metal particles because the various structures and polytypes may have a bearing on the catalytic activity. The stable forms below and above 388 °C are Co(hcp) and Co(fcc), respectively,[46,47] with the two forms coexisting between room temperature and temperatures up to 450 °C because the transformation between them is sluggish.

The actual structure is determined by a number of factors, two of which are particle size and thermal history. Which of the two close-packed structures prevails at room-temperature depends on grain size, small sizes favoring fcc up to 450 °C. The picture is further complicated by a number of polytypes with the fcc and hcp structures constituting the extremes of the range and by the fact that the stacking of the planes within the structure also can be random.[48] The metastable non-close-packed form, Co(bcc), which readily transforms to the close-packed Co(fcc) structure, was first reported by Colley et al.[47] as being the main metal-containing component in the reduced Co/MnO system and also shown to be present in the Co_3O_4/Al_2O_3 system under certain circumstances.[49] Reduction under conditions similar to those used here, but for 13 h, yields first Co(fcc). On cooling to 220 °C and maintaining the catalyst at this temperature for a further 9 h in a 1:1 CO/H_2 mixture, Co(fcc) is largely transformed to Co(bcc). It has been suggested[49] that the presence of interstitial carbon (formed by dissociation of CO) may play an important role in the formation of metastable Co(bcc). Since graphite was present during the reduction (Experimental Section), Co(bcc) has to be considered a possibility but is difficult to substantiate in sample B because the cobalt particles are probably too fine (<40 Å) for X-ray powder diffraction.

Whether or not the metal particles in sample B correspond to the metastable non-close-packed form, Co(bcc), cannot be ascertained from the XAS. Certainly Co(bcc) would exhibit a lower EXAFS amplitude since the coordination of the first shell of neighbors is 8 instead of the 12 for the close-packed forms (hcp and fcc) but this effect would be easily masked by the reduced amplitude arising out of the anharmonic effects of small particle size. XAS is able to distinguish

(48) Shriver, D. F.; Atkins, P. W.; Langford, C. H. *Inorganic Chemistry*; Oxford University Press: Oxford, 1990.
(49) Colley, S. E.; Copperthwaite, R. G.; Hutchings, G. J. *Catal. Today* **1991**, *9*, 203.
(50) Borowski, M. *The 9th International Conference on X-ray Absorption Fine Structure;* 1996; p 148.

between the close-packed and non-close-packed forms for bulklike crystallites. This is demonstrated in Figure 7, which contains the Fourier transform of the XAS of the stable body-centered cubic structure of iron. The differences are clearly discernible: note the shoulder at 2.86 Å due to the cell length. This is the cell dimension (2.86 Å) reported for Co(bcc) so the iron structure is essentially dimensionally identical. For the dimensions involved in sample B the question of structure type may well have become semantic.

Shift in K-Edge Energy. We attribute the edge energy shift in sample B to the small sizes of the cobalt particles. Since a significantly larger fraction of cobalt atoms are either at, or in the proximity of the surface than is the case for bulk crystallites, the properties normally regarded as being representative of the metal are necessarily modified. This also includes the energy of the K-edge. The edge energy (as expressed through the shielding of the 1s electrons by the valence electrons) is a somewhat insensitive probe of chemical environment because the varying extent of expansion or delocalization from the cobalt 3d, 4s, and 4p orbitals into the band structure of the metal affect the shielding properties of these orbitals. The environment of the cobalt atoms, as defined by the crystal structure, determines the band structure. Alterations of this environment are reflected in changes in the band structure which indirectly affect the energy of the 1s level through valence electron shielding. While we can be confident that the high degree of dispersion observed in sample B is associated with cobalt particles small enough to have cobalt electronic environments that deviate from the average of the close-packed bulk metal, we have no evidence for or against any additional contribution from the non-close-packed form Co(bcc). Certainly, the XAS of sample B shows that the energy of the 1s level has increased relative to the bulk. This would seem to indicate an overall decrease in the shielding of the 1s electrons by the valence electron density and that this effect is correlated with small particle size.

Role of Rhenium. In a temperature-programmed reduction (TPR) study of the mechanism of rhenium promotion of alumina-supported cobalt Fischer−Tropsch catalysts, Holmen et al.[28] report that direct contact between rhenium and cobalt particles does not appear to be necessary to promotion. It is suggested that the mechanism by which rhenium promotes the reduction of Co_3O_4 is by hydrogen spillover. It is also reported that cobalt diffuses into the support during the TPR and not during calcination which is what we find. The increased dispersion reported for the reduced rhenium-promoted catalyst relative to the unpromoted catalyst is supported by the small particle sizes found in this XAS study.

Conclusions

XAS shows that high-temperature reduction (450 °C) of rhenium-promoted Co_3O_4/Al_2O_3 yields sample B which contains highly dispersed cobalt in the form of small (<40 Å) metal particles (Co−Co distance 2.49 ± 0.03 Å) together with a minor fraction of cobalt atoms that are randomly spread over the tetrahedral vacancies (Co(II)−O distance 1.92 ± 0.03 Å) of the alumina support. These results are consistent with those of Holmen et al.[26−28] who find that the metal particles constitute 78% of the cobalt content. Also in agreement is the finding that cobalt diffuses into the support during reduction and not during calcination and that this phase is resistant to reduction at 450 °C and is not the spinel $CoAl_2O_4$.

A particularly interesting feature of the XANES of sample B is the 3−4 eV shift of the K-edge to higher energy relative to bulk cobalt metal. This is attributed to an enhanced dispersion of cobalt, relative to the large bulklike crystallites of Co_3O_4 in sample A. Diminished shielding of the 1s electrons by the valence electrons attends this heightened dispersion. The higher dispersion, or smaller particle sizes, in sample B expresses the positive effect that rhenium promotion has on the reducibilty of sample A.

We cannot exclude the possibility that body-centered cobalt metal was formed in sample B, especially since graphite was mixed with the catalyst during the reduction and there is a suggestion that carbon may catalyze the transformation from the hexagonal or face-centered cubic structures to this metastable form of the metal.

Acknowledgment. The Daresbury Laboratory (SRS), UK and HASYLAB, Germany are thanked for providing beamtime. Dr. A. Dent (Daresbury) is thanked for kindly donating the iron data. Support from the Nansen Foundation, the Norwegian Research Council (including a NATO Postdoctoral Fellowship to A. Moen) and VISTA-Statoil is much appreciated. Since the preliminary work (contribution no. 97-5) was carried out at the Swiss-Norwegian Beamline (SNBL) we thank the Norwegian University of Science and Technology and the Norwegian Research Council for grants toward its construction. We also appreciate the assistance of the SNBL Project Team (H. Emerich, P. Pattison, and H. P. Weber). The Danish Natural Science Research Council is also thanked for support to A. Molenbroek.

CM960619T